Journal of Applied Polymer Science

Development of a superporous hydroxyethyl cellulose-based hydrogel by anionic surfactant micelle templating with fast swelling and superabsorbent properties

Xiaoning Shi,[1,2] Jietang,[2] Aiqin Wang[2]

[1]Department of Applied Chemistry, Gansu University of Traditional Chinese Medicine, Lanzhou 730000, China

[2]Center of Eco-Material and Green Chemistry, Lanzhou Institute of Chemical Physics, Chinese Academy of Sciences, Lanzhou 730000, China

Correspondence to: X. N. Shi (E-mail: shixn761128@sina.com)

ABSTRACT: The self-assembling anionic surfactant, sodium *n*-dodecyl sulfonate (SDS) micelles were used as pore-forming templating for fabricating novel superporous hydroxyethyl cellulose-*grafting*-poly(sodium acrylate)/attapulgite (HEC-*g*-PNaA/APT) hydrogels. The network characteristics, morphologies of the hydrogels and removing of SDS micelles from the final product by washing with ethanol/water (v/v, 7 : 3) procedure were determined by Fourier transform infrared spectroscopy and scanning electron microscopy, as well as by determination of swelling ratio, swelling rate, and stimuli response to salts and pHs. The results showed that the added-SDS concentration significantly affected the morphologies and pore structure of the hydrogel, and 2 m*M* SDS facilitates to form a homogeneous and well-defined pore structure in the gel network to extremely improve the swelling ratio and swelling rate. The 2 m*M* SDS-added superporous HEC-based hydrogel not only had highest equilibrium swelling ratio (Q_{eq}, 1118, 102 g g^{-1} in distilled water and 0.9 wt % NaCl solution), rapid swelling rate (k_{is}, 5.2840 g g s^{-1}), also showed multistimulus responses to salts and pHs, which may allow its applications in several areas such as adsorption, separation and biomedical materials. © 2015 Wiley Periodicals, Inc. J. Appl. Polym. Sci. **2015**, *132*, 42027.

KEYWORDS: porous materials; self-assembly; stimuli-sensitive polymers; surfactants; swelling

Received 11 November 2014; accepted 19 January 2015

DOI: 10.1002/app.42027

INTRODUCTION

Exploitation of biomaterials derived from renewable resources is an important approach to address environmental and resource problems in the world today. Polysaccharides-based hydrogels, prepared by free radical graft copolymerization of one or more vinyl functional monomers onto natural polysaccharide backbones in the presence of a cross-linking agent to form three-dimensional polymer network, have been of great interest due to their wide applications in agriculture,[1,2] wastewater treatment,[3,4] hygienic products,[5,6] drug delivery system,[7–9] and tissue engineering,[10–12] etc. These are ascribed to their superabsorbent and their response to changing external conditions, such as temperature, pH, salt, and solvent composition. Another, according to the economical and environmental points of view, polysaccharides-based hydrogels are the most viable, because the biopolymers employed are essentially obtained from natural resources and are biodegradable. However, most of these hydrogels often swell very slowly and may need several hours or days to reach swelling equilibrium. This slow swelling has an obvious limitation in some applications.

The swelling rate of polysaccharides-based hydrogels can be enhanced through the creation of porosity in the network structure and the porous hydrogels have attracted much attention.[13–15] The interconnected porous structure allows the fast diffusion of water molecules into the center of the dried polymer matrix by reducing transport resistance, and endows the hydrogels with additional space to hold more water to enhance swelling capacity. Therefore, creation of porosity in polysaccharides-based hydrogels has been considered as an important process for expanding their applications in many ways. Currently, in accordance with pore-forming mechanism, available techniques for porous hydrogels preparation are porogenation,[16] freeze-drying,[17] emulsion templating,[18,19] and phase separation.[20] Among all these techniques, emulsion templating method can give polymers with well-defined and controllable pore structure through the controlling of emulsion agent concentration.[21,22] Surfactant micelle is one

This article was published online on 12 February 2015. An error was subsequently identified. This notice is included in the online and print versions to indicate that both have been corrected 4 March 2015.

type of templating which is based on the self-assembly of surfactant molecules to form micelles. These micelles can act as a pore-templating in the simultaneous grafting polymerization reaction of natural polysaccharides and vinyl monomer to form porous hydrogels. Sodium *n*-dodecyl sulfate (SDS) is one such surfactant that is known to self-assemble into micelles in water, and has been successfully used to synthesize porous alginate and chitosan-based hydrogels.[23,24]

Cellulose, the most abundant renewable polysaccharide on the earth, has safe, biocompatible, hydrophilic, and biodegradable natures. However, it is insoluble in water and most organic solvent, which limited its application. Hydroxyethyl cellulose (HEC) is known as one of the most important derivatives of cellulose, exhibiting excellent water solubility. Its unique properties make it easily grafting polymerization with hydrophilic vinyl monomers through the abundant reactive –OH groups on the HEC backbones in aqueous solution to formulate new materials. Among the various vinyl monomers, acrylic acid (AA) is a commercially important monomer that has been widely used in the preparation of functional cellulose derivatives-based hydrogels. The incorporation of carboxyl groups into the natural polymer network, which imparts cellulose derivatives-based hydrogels response to various external stimuli, such as salts and pHs, and thus allows their use not only in water adsorption to selective removal of heavy metal ions or dyes, but in drug release systems. Several cellulose derivative-*grafting*-poly(acrylic acid) hydrogels have been reported.[25–27] In the present work, we prepared novel superporous hydroxyethyl cellulose-*grafting*-poly(sodium acrylic)/attapulgite (HEC-*g*-PNaA/APT) hydrogel using an anionic surfactant SDS micelles as the pore-forming templating. Fourier transform infrared (FTIR) spectra were used to confirm the successful synthesis of HEC-*g*-PNaA/APT hydrogel and removal of SDS micelles from the final products by the ethanol/water mixture solution washing process. The effect of SDS concentration on the morphologies and pore structure of the hydrogels was characterized by Scanning electron microscope, and effects of SDS concentration on the equilibrium swelling ratio and swelling rate were also investigated to optimize the synthesis condition. In addition, the multistimulus responses of the superporous HEC-based hydrogel to salts and pH were also evaluated systematically.

EXPERIMENTAL

Materials

Materials for the superporous hydrogel synthesis: Hydroxyethyl cellulose (HEC), *N*,*N*′-methylenebisacrylamide (MBA, AR), and SDS were purchased from Shanghai chemical reagents Corp. (Shanghai, China); Acrylic acid (AA, CP) was purchased from Shanghai Wulian Chemical Factory (Shanghai, China); Ammonium persulfate (APS, AR) was purchased from Xi'an Chemical Reagent Factory (Xi'an, China). Attapulgite clay (APT, milled and passed through a 320-mesh screen prior to use) was supplied by Gaojiawa Colloidal Co. (Jiangsu, China). All other chemicals were of analytical grade and all solutions were prepared with distilled water.

Preparation of the Superporous Hydrogel

The general procedure for the synthesis superporous HEC-*g*-PNaA/APT hydrogel via anionic surfactant SDS micelles templating is follow: 1.20 g HEC powder was uniform dispersed in 30 mL distilled water in a 250 mL four-necked round bottom flask. Then, a proper amount of SDS aqueous solution was added to the flask. The resulting mixture was stirred with a mechanical stirrer at 300 rpm for 15 min to obtain a homogeneous solution. The equipment was preheated in a water bath to 65°C and flushed with nitrogen to remove the dissolving oxygen, 5 mL APS solution (0.100 g) was added and kept at 65°C for 15 min to generation radicals. Afterward, the reaction system was cooled to 40°C, to which a mixture of AA (7.20 g, 70% neutralized degree), APT (0.928 g) as well as crosslinker MBA (0.0216 g) was added. The reaction temperature was risen to 70°C and then maintained for 3 h to complete the polymerization reaction. The hydrogel was taken out and firstly immersed in ethanol/water solution (v/v, 7 : 3) to remove SDS, and then dehydrated by absolute ethanol. The dried product was ground and passed through 40∼80 meshes (the particle size is 180∼380 μm).

The compared non-porous HEC-*g*-PNaA/APT hydrogel was also prepared by the above method but without SDS.

Swelling Studies

The gravimetric method was employed to measure the swelling ratio of the superporous hydrogels in distilled water, salt solutions and different pH solutions. The swelling temperature was set as room temperature for exploring potential environmental applications. The buffer solutions with various pH values were prepared by mixing KH_2PO_4, K_2HPO_4, H_3PO_4, and NaOH properly, and the ionic strengths were controlled to 0.1 *M* using NaCl. The pH values were determined by a pH-meter (Mettler Toledo, ±0.1). The equilibrium swelling ratio (Q_{eq}; g g^{-1}) was determined according to the following equation:

$$Q_{eq} = (m_s - m_d)/m_d \quad (1)$$

where m_s was the mass of the swollen hydrogels (g) and m_d was the mass of the hydrogels in the dry state (g). The data points represent mean ± standard deviation from three repeated experiments.

The swelling kinetics of the superporous hydrogels in the above swelling media was measured gravimetrically. At predetermined time intervals (1, 3, 5, 7, 10, 15, 20, 30, 60, and 120 min), the swollen hydrogels were taken out from the swelling medium and weighed after removing the excess water on the surface, Q_t values were estimated according to eq. (1), correlating the mass of the swollen hydrogels (m_t) at given time t to the dry hydrogels (m_d).

Instrumental Analysis

FTIR spectra of samples were taken in KBr pellets using Nicolet NEXUS FTIR spectrometer within the frequency range of 400–4000 cm^{-1}. The surface morphologies of the xerogels were investigated using *S*−4800 scanning electron microscope instrument (Japan) after sputter coating the samples with gold film.

RESULTS AND DISCUSSION

Mechanism for the Formation of Superporous HEC-g-PNaA/APT Hydrogel

A proposed mechanism for the formation of superporous HEC-*g*-PNaA/APT hydrogel by anionic surfactant SDS micelle templating is shown in Scheme 1. Firstly, an aqueous SDS solution

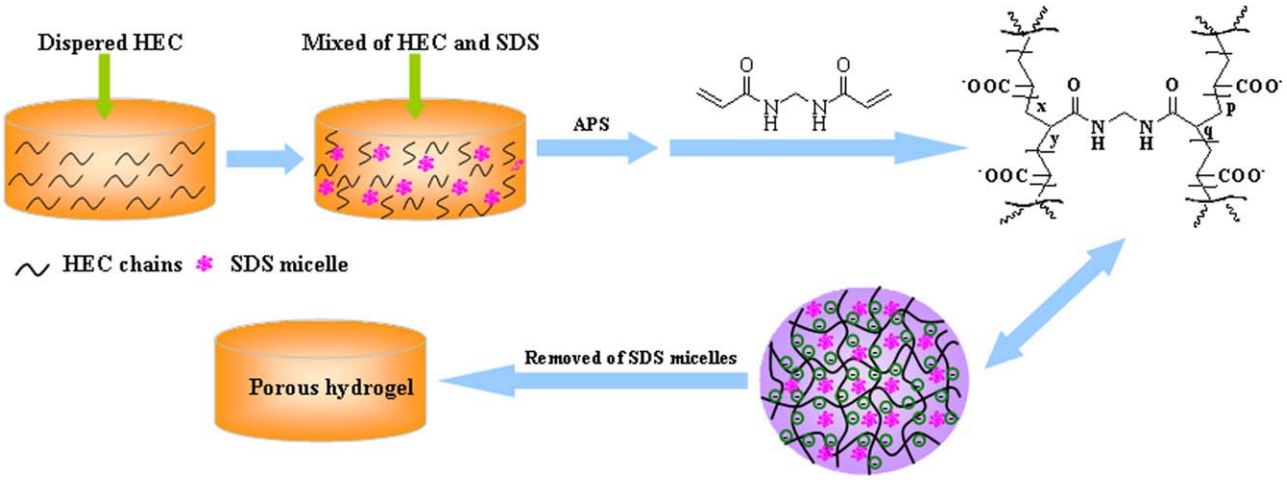

Scheme 1. A proposed mechanism for the preparation of superporous HEC-*g*-PNaA/APT hydrogel. [Color figure can be viewed in the online issue, which is available at wileyonlinelibrary.com.]

was added in the dispersed HEC mixture to form SDS micelles by the self-assembling of SDS molecules. Then, sulfate anion radicals generated from heating decomposed APS extract hydrogen from –OH groups of the HEC backbones to form alkoxy radicals. The monomer molecules, AA/NaA, which closed to this active centers on the HEC backbones, became acceptor of HEC radicals resulting in chain initiation to grafting and polymerization. At the present of crosslinker MBA, the end vinyl groups of MBA may react synchronously with polymer chains to form a chemical crosslinked 3D-structure. At the same time, the inorganic nanoclay APT also acted and chemically combined in this network through its active Si-OH. In the above grafting copolymerization and crosslinking process, the self-assembled SDS micelles may be physically enclosed in the polymeric network. After removed SDS micelles by ethanol/water washing procedure, the superporous structure was generated in the hydrogel network.

Characterization of Superporous HEC-g-PNaA/APT Hydrogel by FTIR

FTIR spectroscopy was utilized to confirm the chemical structure of HEC-*g*-PNaA/APT hydrogel. Figure 1 shows the FTIR spectra of (a) HEC, (b) APT, and (c) ethanol/water washed HEC-*g*-PNaA/APT hydrogel in the spectral range of 4000–500 cm^{-1}. In spectrum (a), the characteristic absorption bands at 1465, 1372, 1169, 1124, 1051 cm^{-1} are related to the C–H and C–O bond stretching frequencies of the HEC backbones, which were obviously shifted and weakened after reaction. In spectrum (c), new bands at 1725, 1577, 1455, and 1411 cm^{-1} are related to the stretching vibration of C═O, asymmetric stretching vibration, and symmetric stretching vibration of $–COO^-$ groups, respectively. The position of these bands is close to that of PNaA, which revealed that NaA was grafted onto HEC backbone.[25] In addition, in spectrum (b), the (Al)O–H stretching vibration at 3615 cm^{-1}, (Si)O–H stretching vibration at 3545 cm^{-1} and the –OH bending vibration at 1647 cm^{-1} disappeared in the spectrum of (c). However, the ≡Si–O stretching vibration of APT at 1031 cm^{-1} still appeared in the spectrum of HEC-*g*-PNaA/APT hydrogel with a weakened intensity [Figure 1(c)]. The above information indicated that APT participated in the graft copolymerization reaction through its active silanol groups and chemically bond with the polymer chains.[28]

FTIR spectroscopy also was employed to confirm that SDS micelles only acted as pore-forming templating, which could be removed from the hydrogel network (Figure 2). The synthesized hydrogels were dried by two methods: one is directly oven-dried

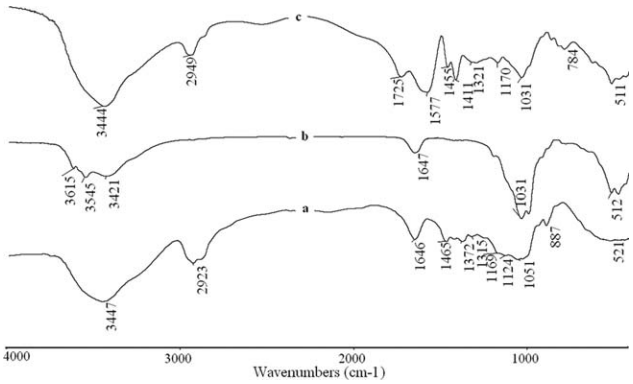

Figure 1. FTIR spectra of (a) HEC, (b) APT, and (c) ethanol/water (v/v, 7 : 3) washed HEC-*g*-PNaA/APT hydrogel.

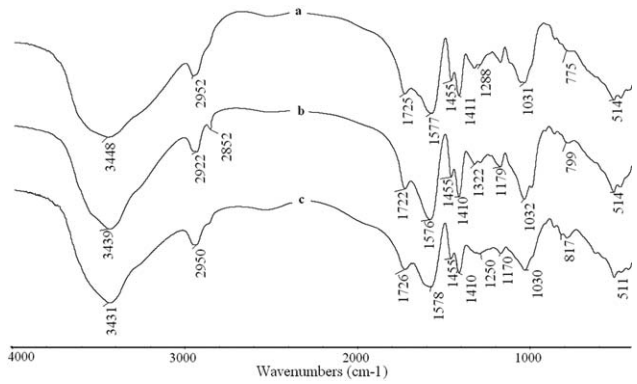

Figure 2. FTIR spectra of (a) non-SDS-added hydrogel, (b) nonwashed-SDS hydrogel, and (c) washed-SDS hydrogel

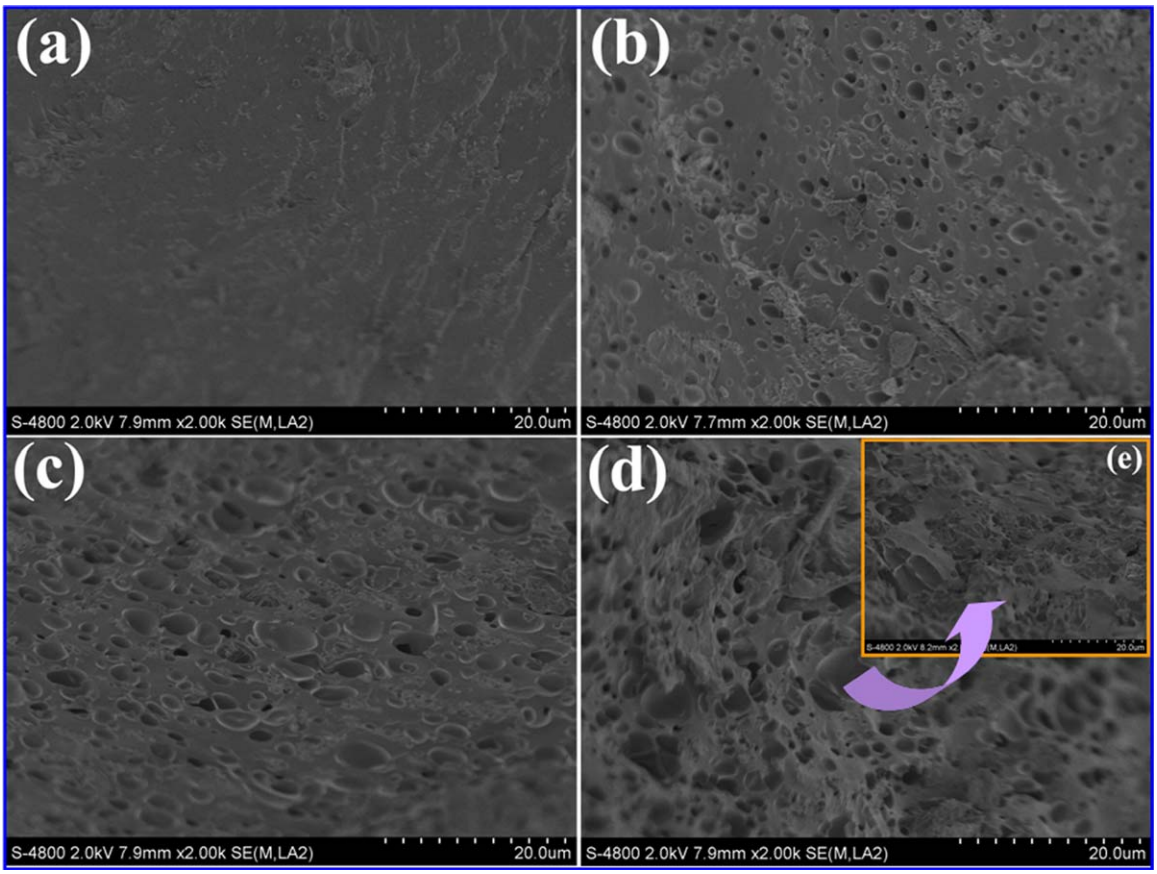

Figure 3. SEM photographs of the HEC-*g*-PNaA/APT hydrogels prepared with (a) 0 m*M*, (b) 1 m*M*, (c) 2 m*M*, (d) 3 m*M*, and (e) 4 m*M* SDS. [Color figure can be viewed in the online issue, which is available at wileyonlinelibrary.com.]

at 70°C; the other is completely soaked in ethanol/water (v/v, 7 : 3) solution for 24 h and then dehydrated by absolutely alcohol. In the oven-dried sample spectra [Figure 2(b)], the typical peaks appearing around 2852, 1179, and 1322 cm^{-1}, were assigned to C–H stretching vibration of $–CH_2–$,[25] O═S═O symmetrical and asymmetrical stretching vibration of the sulfonate groups, respectively, of SDS molecules.[29] These peaks disappeared or weakened after the hydrogel was washed with ethanol/water solution [Figure 2(c)]. In addition, the profiles of the characteristic absorption peaks for SDS-free [Figure 2(a)] and washed-SDS hydrogels are almost identical, implying that all residual SDS have been removed from the hydrogel network.

Surface Morphology Analysis

Scanning electron microscopy (SEM) was used to assess the influence of SDS micelles on the surface morphology and microstructure of the HEC-*g*-PNAa/APT hydrogel. As presented in Figure 3(a), no porosity was observed on the surface of SDS-free sample, although it is not completely smooth. The porosity structure was occurred in the SDS-added samples and displayed a gradual change in the pore density [Figure 3(b–d)]. It is obvious that the pores of 1 m*M* SDS-added sample were scattered and 2 m*M* SDS-added sample developed a continuous skin enveloped the skeleton of a macroporous interior. Thickness of the skin decreased with increasing SDS concentration, which lead to the porous skeletons of the hydrogels were more fragile and easy to collapse [Figure 3(d,e)]. The related procedural reasons can be explained as follows. The pores of the hydrogel is mainly due to the self-assembling of SDS molecules in aqueous environment and the non-spherical micelles act as pore-forming templating.[21] At lower concentration (1 m*M* SDS), it mostly existed as dissociative ions and not enough micelles used as pore-forming templating, and the pore network

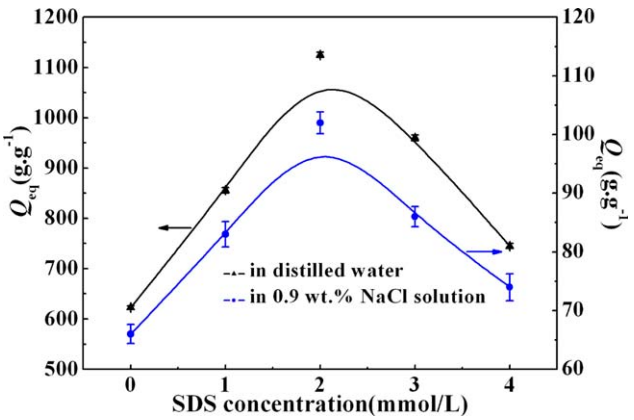

Figure 4. Influence of SDS concentrations on Q_{eq} of the superporous HEC-*g*-PNaA/APT hydrogels. [Color figure can be viewed in the online issue, which is available at wileyonlinelibrary.com.]

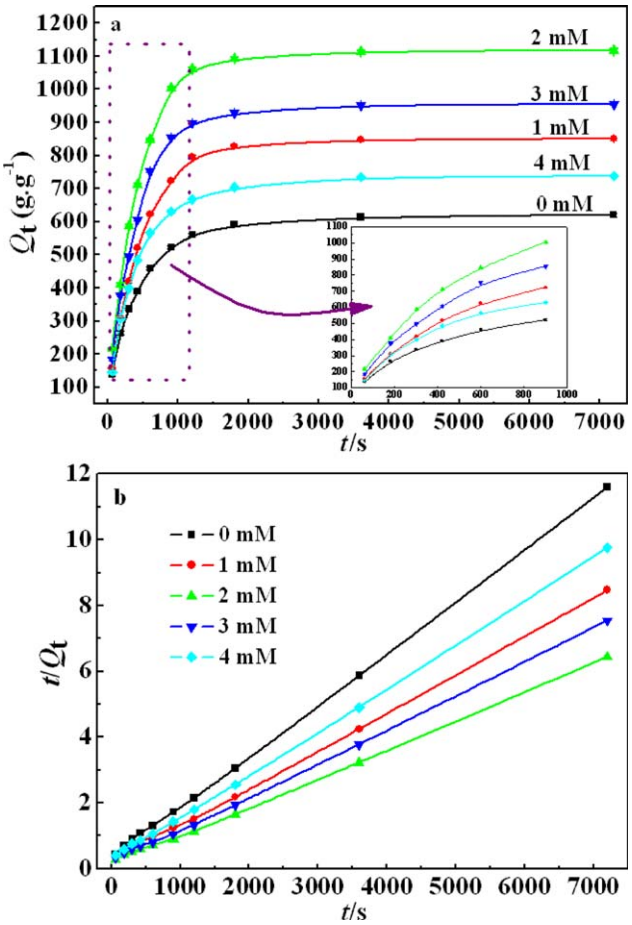

Figure 5. Time-dependent swelling behaviors of the superporous HEC-*g*-PNaA/APT hydrogels generated by different concentration of SDS in distilled water (a) and their t vs. t/Q_t graphs according to eq. (2) (b). [Color figure can be viewed in the online issue, which is available at wileyonlinelibrary.com.]

appeared to scatter. With increasing SDS concentration (2 m*M*), micelles can be formed more easily, and act as pore-templating in the gelling process to generate regular porous structure [Figure 3(c)]. However, when the SDS concentration was higher than 4 m*M*, the hydrogel display a collapsed network and is too fragile to be handled. It may be a high concentration of surfactant possibly interfered with the gelling mechanism and restricts the formation of the 3D network.[23]

Influence of SDS Concentration on the Swelling Ratio and Swelling Rate

The direct information about the structure and morphology of the hydrogels can be provided by swelling studies.[30] Figure 4 demonstrates the influence of SDS concentration on Q_{eq} of the HEC-*g*-PNaA/APT hydrogels in distilled water and 0.9 wt % NaCl solution. It was observed that Q_{eq} is firstly increased with increasing SDS concentration from 0 to 2 m*M*, reached a maximum Q_{eq} (1118, 102 g g^{-1} in distilled water and 0.9 wt % NaCl solution, respectively) at 2 m*M* SDS and then decreased with the further increase in SDS concentration. It is supposed that the pores are the regions of water permeation and interaction sites

Table I. The Swelling Kinetic Parameters of the Superporous HEC-*g*-PNaA/APT Hydrogels Calculated According to eq. (2)

Samples	Q_{eq} (g·g^{-1})	Q_∞ (g·g^{-1})	k_{is} (g·g^{-1}·s^{-1})	R
0	621	645	2.8376	0.9998
1	850	885	3.5881	0.9994
2	1118	1163	5.2840	0.9993
3	954	990	4.6307	0.9995
4	737	763	3.4708	0.9998

of external stimuli with the hydrophilic groups of the hydrogels. Proper concentration of SDS is reasoned to produce homogeneous pore structure and increase the spaces for water storage [see Figure 3(c)], and consequently resulting Q_{eq} is improved. However, a much looser network is easily collapsed when the hydrogels are subjected to swelling and, thus, shows decreasing Q_{eq}. This well agrees with the results obtained from SEM.

To test the swelling rate we measured the time-dependent swelling behaviors of the superporous hydrogels in distilled water. The results shown in Figure 5(a) indicated that the swelling rate of the hydrogels was significantly influenced by SDS concentration. Schott had proposed a theoretical second-order swelling kinetics model to investigate the controlling mechanism of the hydrogel swelling process, which was described in the form of the following equation:[31]

$$\frac{t}{Q_t} = \frac{1}{k_s Q_\infty^2} + \frac{1}{Q_\infty} t \qquad (2)$$

where Q_∞ was the theory equilibrium swelling ratio, k_s was the swelling rate constant, which depended on the initial swelling rate k_{is} ($=k_s Q_\infty^2$) and Q_∞. To test this kinetics model, the reciprocal of the average swelling rate (t/Q_t) and the swelling time (t) shows a good straight linear regression [Figure 5(b)], indicating that the swelling process of the study hydrogels followed Schott's second-order swelling model. The kinetic parameters Q_∞ and k_{is} could be calculated from the slopes and intercepts

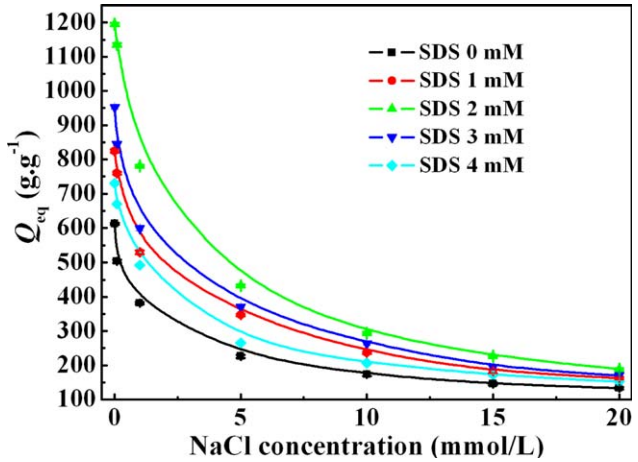

Figure 6. Swelling behaviors of the superporous HEC-*g*-PNaA/APT hydrogels generated by different SDS concentration in various concentrations of NaCl solution. [Color figure can be viewed in the online issue, which is available at wileyonlinelibrary.com.]

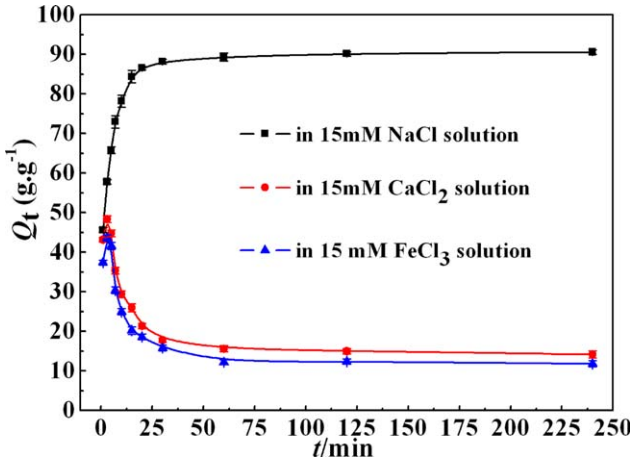

Figure 7. Time-dependent swelling behaviors of 2 m*M* SDS-added superporous hydrogel in 15 m*M* NaCl, $CaCl_2$, and $FeCl_3$ solutions. [Color figure can be viewed in the online issue, which is available at wileyonlinelibrary.com.]

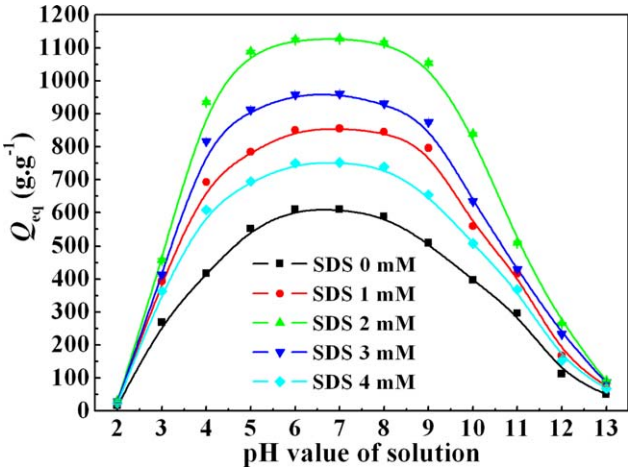

Figure 8. Q_{eq} of the superporous HEC-*g*-PNaA/APT hydrogels generated by different concentration of SDS in pH 2–13 solutions. [Color figure can be viewed in the online issue, which is available at wileyonlinelibrary.com.]

of the above lines and tabulated in Table I. It was shown that the values of k_{is} increased with increasing SDS concentration from 0 to 2 m*M*, but decreased with its further increasing. Generally, the initial swelling rate was related to a solvent diffusion rate and relaxation rate of polymer chains.[32] The homogeneous pore structure of the polymer network not only contribute to enlarge specific surface area to speed up the diffusion rate but also provide the open channel essential for faster water absorption. The obviously improved k_{is} value for 2 m*M* SDS-added sample further confirmed that the proper concentration of SDS micelles attributed to act as pore-forming templating to produce superporous HEC-based hydrogel with fast swelling.

Salt-Responsive Behaviors

It is important for hydrogels to have high swelling ratio in salt solution for expanding their applications in the environmental field. The swelling behaviors of superporous HEC-based hydrogels generated by different SDS concentration in various concentrations of NaCl solution are shown in Figure 6. As expected, the Q_{eq} of the hydrogels firstly increased with an increase in SDS concentration and the maximum swelling ratio was obtained when the concentration of SDS is 2 m*M*. This confirmed further that 2 m*M* is the best concentration for producing regular pore structure to accommodate more water either in distilled water or NaCl solution. Moreover, the Q_{eq} of all hydrogel samples decreased with increasing of salt concentration. The swelling and shrinking behaviors of the hydrogels in salt solution can be determined by the ionic interactions between mobile ions and the fixed charges which make great contribution to the Donnan osmotic pressure between the interior network of the hydrogel and the exterior solution.[33] With the increasing of Na^+ concentration, the shrinking of hydrogels is mainly due to the decreasing of Donnan osmotic pressure.

Furthermore, the swelling kinetics of 2 m*M* SDS-added sample in 15 m*M* NaCl, $CaCl_2$ and $FeCl_3$ are shown in Figure 7. It is observed that the swelling kinetic behaviors strongly depended on the "type" of salt added to the swelling medium. The water absorption of the hydrogel in NaCl solution increased with prolonging swelling time until reached the equilibrium, which is similar to the swelling kinetics curve in distilled water. However, in $CaCl_2$ and $FeCl_3$ solutions, the water absorption firstly increased within 7 min and reached a maximum swelling ratio (35, 30 g g^{-1} in $CaCl_2$ and $FeCl_3$ solutions, respectively), and then gradually decreased to a constant value. This time-

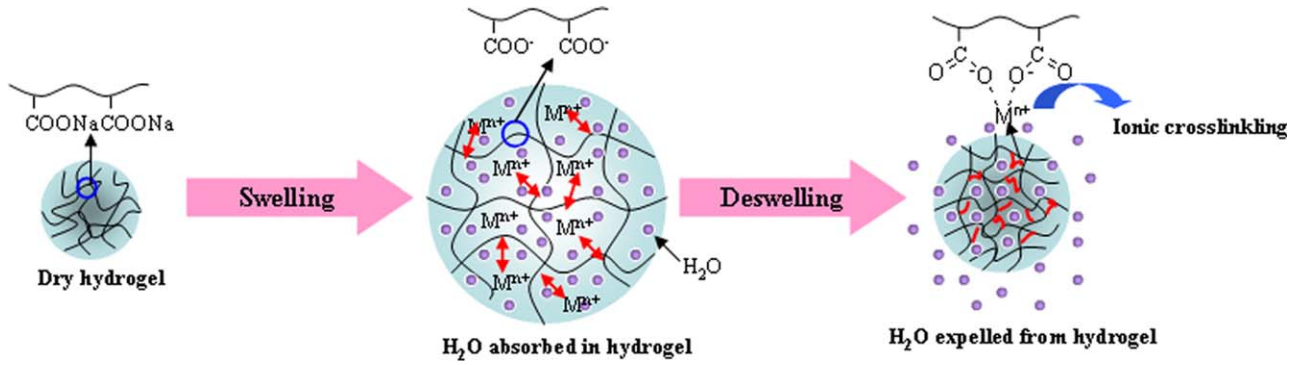

Scheme 2. A schematic diagram of the swelling process with "overshooting effect" in 15 m*M* $CaCl_2$ and $FeCl_3$ solutions. [Color figure can be viewed in the online issue, which is available at wileyonlinelibrary.com.]

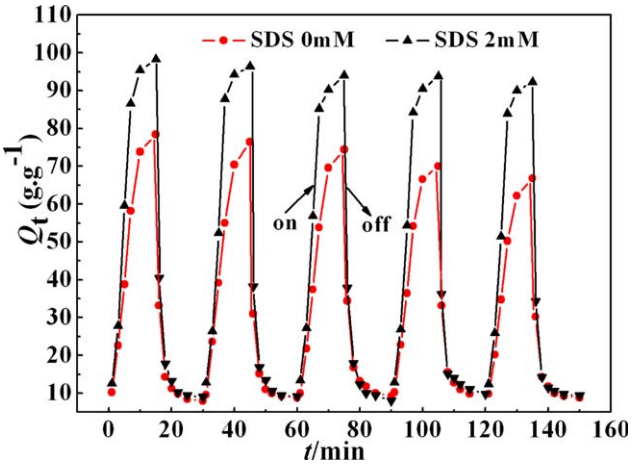

Figure 9. The reversible pH-controlled on–off switching for 0 and 2 m*M* SDS-added hydrogels in pH 2.2 and 7.4 buffer solutions. [Color figure can be viewed in the online issue, which is available at wileyonlinelibrary.com.]

dependent swelling-shrinking phenomenon is known as "overshoot effect,"[34] which could be depicted in Scheme 2. Upon contact with swelling medium, hydrogen-bonding interaction forces are established between the hydrogel and swelling medium, introducing the water molecules into the hydrogel network voids to expand the hydrogel network. As a result, the expanded hydrogel network accelerates the diffusion of Ca^{2+} and Fe^{3+} into gel network, and then complex with $–COO^-$ groups. The stronger ionic complexing increased the crosslinking point in the hydrogel network interior, and caused the shrinkage of swollen hydrogel. When the expansion and contraction of the hydrogel network are equal, the hydrogel reached a swelling equilibrium state. In view of the above results, the lower swelling ratio of the hydrogel in multivalence salt solution than in NaCl solution is mainly due to ionic complexing.

pH-Responsive Behaviors

The pH-responsive behavior of the hydrogel is based on the chargeable groups present in the network.[35] Figure 8 shows the Q_{eq} of hydrogels with different SDS concentration as a function of pH values. The observed swelling behavior similar with most of the ones reported in the literatures.[36,37] The Q_{eq} values of the hydrogels were lower than 16.0 g g^{-1} at pH 2.0 and then rapidly increased to pH 6.0. One possible explanation for the shrinking/swelling state of the hydrogels in different pH solutions is the conversion of $–COO^-$ and –COOH groups in the gel structure. The pK_a value of the carboxylic group is 4.6, $–COO^-$ groups are gradually protonated and transformed into –COOH groups at pH < 4.6 solutions. The protonation of $–COO^-$ groups, on the one hand, results in a decrease in the electrostatic repulsion among negatively charged $–COO^-$ groups, on the other hand, strengthen the hydrogen-bonding crosslinking interaction among –COOH groups and, thus, the shrinking of the gel network. However, when the solution of pH is higher than 4.6, the deprotonation of –COOH groups occurs, which leads to strong electrostatic repulsion to expand gel network and improve the Q_{eq} Again, a charge screening effect of the counter ions (Na^+) limits the swelling at pH >10 and the ESR decreased.

The modulation of the pH values in which hydrogels present shrinking/swelling state is an outstanding feature being useful in many biological applications. Figure 9 shows the reversible pH-controlled on–off switching when the hydrogels were exposed to buffer solutions of pH 2.2 (off) and 7.4 (on). It can be noticed that the swollen hydrogels in pH 7.4 solution rapidly shrinks in pH 2.2 solution and a prominent reversible on-off switch can be achieved within 30 min. After five swelling-shrinking cycles, this intriguing on–off switching is still observed. Additional, the above pH-controlled switch for 2 m*M* SDS-added sample is more prominent as compared with non-SDS-added sample, which is reflected by the higher and lower swelling ratios with the switch on and off, respectively.

CONCLUSIONS

In this work, novel superporous HEC-*g*-PNaA/APT hydrogel was developed using the simultaneous SDS micelles templating and internal grafting polymerization. The grafting polymerization of HEC, NaA, and APT was confirmed by FTIR spectra and the mechanistic pathway for the formation of superporous HEC-*g*-PNaA/APT hydrogel by anionic surfactant SDS micelles templating was proposed. The added SDS concentration significantly affected the morphologies and pore structure of the hydrogels, which characterized by SEM. The 2 m*M* SDS facilitates to form a homogeneous and well-defined pore structure in gel network to extremely improve the swelling ratio and swelling rate. The prepared superporous HEC-based hydrogel exhibited smart salt and pH responsive behaviors. Their swelling ratio decreased with an increase in the salt concentration on the whole, and was more sensitive to multivalence ions (e.g., Ca^{2+} and Fe^{3+}), which is due to stronger ionic complexing and a more prominent charge screen effect. In addition, the superporous structure of the hydrogel became easily expanded in the solutions at pH 5∼9, whereas shrinkage occurred when the hydrogel was exposed to low pH (<4) solutions, and the hydrogel showed reversible on–off switching behavior in pH 2.2 and 7.4 buffer solutions. This superporous HEC-based hydrogel with higher swelling ratio, faster swelling rate, and multistimulus response properties could be useful for wide applications, including agriculture, foods, biomedical, and other industrial fields.

ACKNOWLEDGMENTS

The authors gratefully acknowledge jointly supporting of this research by the Youth Fund Project of Gansu University of Traditional Chinese Medicine (2305016601), the Science and Technology Support Project of Jiangsu Provincial Sci. & Tech. Department (No. BY2010012) and the National Natural Science Foundation of China (No. 21377135).

REFERENCES

1. Wang, X. G.; Lü, S. Y.; Gao, C. M.; Xu, X. B.; Zhang, X. J.; Bai, X.; Liu, M. Z.; Wu, L. *Chem. Eng. J.* **2014**, *252*, 404.
2. Rashidzadeh, A.; Olad, A. *Carbohydr. Polym.* **2014**, *114*, 269.
3. Paulino, A. T.; Belfiore, L. A.; Kubota, L. T.; Muniz, E. C.; Tambourgi, E. B. *Chem. Eng. J.* **2011**, *168*, 68.

4. Dragan, E. S.; Lazar, M. M.; Dinu, M. V.; Doroftei, F. *Chem. Eng. J.* **2012**, *204*, 198.
5. Marsich, E.; Travan, A.; Donati, I.; Luca, A. D.; Benincasa, M.; Crosera, M.; Paoletti, S. *Colloids Surf. B: Biointerfaces* **2011**, *83*, 331.
6. Halake, K. S.; Lee, J. *Carbohydr. Polym.* **2014**, *105*, 184.
7. Matricardi, P.; Meo, C. D.; Coviello, T.; Hennink, W. E.; Alhaique, F. *Adv. Drug Deliv. Rev.* **2013**, *65*, 1172.
8. Singh, B.; Bala, R. *Int. J. Biol. Macromol.* **2014**, *65*, 524.
9. Singh, B.; Chauhan, N.; Kumar, S. *Carbohydr. Polym.* **2008**, *73*, 446.
10. Tiwari, A.; Grailer, J. J.; Pilla, S.; Steeber, D. A.; Gong, S. *Acta Biomater.* **2009**, *5*, 3441.
11. Stalling, S. S.; Akintoye, S. O.; Nicoll, S. B. *Acta Biomater.* **2009**, *5*, 1911.
12. Suekama, T. C.; Hu, J.; Kurokawa, T.; Gong, J. P.; Gehrke, S. H. *ACS Macro Lett.* **2013**, *2*, 137.
13. Kuang, J.; Yuk, K. Y.; Huh, K. M. *Carbohydr. Polym.* **2011**, *83*, 284.
14. Yom-Tov, O.; Neufeld, L.; Seliktar, D.; Bianco-Peled, H. *Acta Biomater.* **2014**, *10*, 4236.
15. Dragan, E. S.; Apopei, D. F. *Carbohydr. Polym.* **2013**, *92*, 23.
16. Zamani, A.; Henriksson, D.; Taherzadeh, M. J. *Carbohydr. Polym.* **2010**, *80*, 1091.
17. Autissier, A.; Visage, C. L.; Pouzet, C.; Chaubet, F.; Letourneur, D. *Acta Biomater.* **2010**, *6*, 3640.
18. Zhao, B.; Moore, J. S. *Langmuir* **2001**, *17*, 4758.
19. Monteiro, M. J.; Hall, G.; Gee, S.; Xie, L. *Biomacromolecules* **2004**, *5*, 1637.
20. Pradas, M. M.; Ribelles, J. L. G.; Aroca, A. S.; Ferrer, G. G.; Antón, J. S.; Pissis, P. *Polymer* **2001**, *42*, 4667.
21. Partap, S.; Muthutantri, A.; Rehman, T. U.; Davis, G. R; Darr, J. A. *J. Mater. Sci.* **2007**, *42*, 3502.
22. Marras-Marquez, T.; Peña, J.; Veiga-Ochoa, M. D. *Carbohydr. Polym.* **2014**, *103*, 359.
23. Su, J. C.; Liu, S. Q.; Joshi, S. C.; Lam, Y. C. *J. Therm. Anal. Calorim.* **2008**, *93*, 495.
24. Chatterjee, S.; Chatterjee, T.; Woo, S. H. *Bioresour. Technol.* **2010**, *101*, 3853.
25. Wang, W. B.; Wang, A. Q. *Carbohydr. Polym.* **2010**, *82*, 83.
26. Chang, C. Y.; Duan, B.; Cai, J.; Zhang, L. N. *Eur. Polym. J.* **2010**, *4*, 92.
27. Liu, J.; Li, Q.; Su, Y.; Yue, Q. Y.; Gao, B. Y.; Wang, R. *Carbohydr. Polym.* **2013**, *94*, 539.
28. Zhang, J. P.; Wang, Q.; Wang, A. Q. *Carbohydr. Polym.* **2007**, *68*, 367.
29. Pourjavadi, A.; Hosseinzadeh, H.; Mahdavinia, G. R.; Farhadpour, B. *Polym. Compos.* **2007**, *15*, 43.
30. Pourjavadi, A.; Kurdtabar, M. *Eur. Polym. J.* **2007**, *4*, 877.
31. Schott, H. *J. Macromol. Sci. B* **1992**, *31*, 1.
32. Zhan, Y.; Tan, T. W.; Kinoshita, T. *J. Polym. Sci. Part B: Polym. Phys.* **2010**, *48*, 666.
33. Demitri, C.; Sole, R. D.; Scalera, F.; Sannino, A.; Vasapollo, G.; Maffezzoli, A.; Ambrosio, L.; Nicolais, L. *J. Appl. Polym. Sci.* **2008**, *110*, 2453.
34. Lee, W. F.; Wum, R. J. *J. Appl. Polym. Sci.* **1996**, *62*, 1099.
35. Zohuriaan-Mehr, M. J.; Motazedi, Z.; Kabiri, K.; Ershad-Langroudi, A.; Allahdadi, I. *J. Appl. Polym. Sci.* **2006**, *102*, 5667.
36. Peng, X. W.; Ren, J. L.; Zhong, L. X.; Peng, F.; Sun, R. C. *J. Agric. Food Chem.* **2011**, *59*, 8208.
37. Witono, J. R.; Noordergraaf, I. W.; Heeres, H. J.; Janssen, L. P. B. M. *Carbohydr. Polym.* **2014**, *103*, 325.